

Multiple regression analysis of anthropogenic and heliogenic climate drivers, and some cautious forecasts

Frank Stefani^a

^aHelmholtz-Zentrum Dresden-Rossendorf, Institute of Fluid Dynamics, Bautzner Landstr. 400, 01328 Dresden, Germany

ARTICLE INFO

Keywords:
Climate change
Solar cycle
Forecast

ABSTRACT

The two main drivers of climate change on sub-Milankovic time scales are re-assessed by means of a multiple regression analysis. Evaluating linear combinations of the logarithm of carbon dioxide concentration and the geomagnetic aa-index as a proxy for solar activity, we reproduce the sea surface temperature (HadSST) since the middle of the 19th century with an adjusted R^2 value of around 87 per cent for a climate sensitivity (of TCR type) in the range of 0.6 K until 1.6 K per doubling of CO_2 . The solution of the regression is quite sensitive: when including data from the last decade, the simultaneous occurrence of a strong El Niño on one side and low aa-values on the other side lead to a preponderance of solutions with relatively high climate sensitivities around 1.6 K. If those later data are excluded, the regression leads to a significantly higher weight of the aa-index and a correspondingly lower climate sensitivity going down to 0.6 K. The plausibility of such low values is discussed in view of recent experimental and satellite-borne measurements. We argue that a further decade of data collection will be needed to allow for a reliable distinction between low and high sensitivity values. Based on recent ideas about a quasi-deterministic planetary synchronization of the solar dynamo, we make a first attempt to predict the aa-index and the resulting temperature anomaly for various typical CO_2 scenarios. Even for the highest climate sensitivities, and an unabated linear CO_2 increase, we predict only a mild additional temperature rise of around 1 K until the end of the century, while for the lower values an imminent temperature drop in the near future, followed by a rather flat temperature curve, is prognosticated.

1. Introduction

As heir of its great pioneers Arrhenius (1906) and Callendar (1938), modern climate science (Knutti *et al.*, 2017) has been surprisingly unsuccessful in narrowing down its most prominent parameter - equilibrium climate sensitivity (ECS) - from the ample range 1.5 K-4.5 K (per $2\times\text{CO}_2$) as already given in the report by Charney (1979). This sobering scientific yield is often discussed in terms of various interfering socio-scientific and political factors (Hart, 2015; Lindzen, 2020; Vahrenholt and Lüning, 2020). Yet, in addition to those more “subjective” reasons for climate science to be that *unsettled*, there are at least two “objective” ones: the lack of precise and reliable experimental measurements of the climate sensitivity until very recently, and the unsatisfying state of understanding the complementary solar influence on the climate. Certainly, a couple of mechanisms have been proposed (Hoyt and Schatten, 1993; Gray *et al.*, 2010; Lean, 2010) that could significantly surmount the meager 0.1 per cent variation of the total solar irradiance (TSI) which is routinely used as an argument against any discernible solar impact on the climate. Among those mechanisms, the following ones figure most prominently: the comparable large variation of the UV component with its influence on the ozone layer and the resulting stratospheric-tropospheric coupling (Labitzke and van Loon, 1988; Haigh, 1994; Soon, Posmentier and Baliunas, 2000; Georgieva *et al.*, 2012; Silverman *et al.*, 2018; Veretenenko and Ogurtsov, 2020); the effects of solar magnetic field modulated cosmic

rays on aerosols and clouds (Svensmark and Friis-Christensen, 1997; Soon *et al.*, 2000; Shaviv and Veizer, 2003; Svensmark *et al.*, 2017); downward winds following geomagnetic storms in the polar caps of the thermosphere, penetrating stratosphere and troposphere (Bucha and Bucha, 1998); solar wind’s impact on the global electric current (Tinsley, 2000, 2008); and the (UV) radiation effects on the growth of oceanic phytoplankton (Vos *et al.*, 2004) which, in turn, produces dimethylsulphide, a major source of cloud-condensation nuclei (Charlson *et al.*, 1987). But even the very TSI was claimed (Hoyt and Schatten, 1993; Scafetta and Willson, 2014; Egorova *et al.*, 2018; Connolly *et al.*, 2021) to have risen much more steeply since the Little Ice Age than assumed in the conservative estimations by Wang, Lean and Sheeley (2005); Steinhilber, Beer and Fröhlich (2009); Krivova, Vieira and Solanki (2010). While neither of those mechanism can presently be considered as conclusively proven (Solanki *et al.*, 2002; Courtillot *et al.*, 2007; Gray *et al.*, 2010), they all together entail significantly more potential for solar influence on the terrestrial climate than what was discussed on the corresponding one and a half pages of Bindoff *et al.* (2013).

In view of illusionary claims (Cook *et al.*, 2016) of an overwhelming scientific consensus on this complex and vividly debated research topic, and the severe political consequences drawn from it, we reiterate here Eugene Parker’s prophetic warning (Parker, 1999) that “...it is essential to check to what extend the facts support these conclusions before embarking on drastic, perilous and perhaps misguided plans for global action”. We also agree with his “...inescapable conclusion (...) that we will have to know a lot more about the sun and the terrestrial atmosphere before we can understand the na-

✉ F. Stefani@hzdr.de (F. Stefani)
ORCID(s): 0000-0002-8770-4080 (F. Stefani)

ture of contemporary changes in climate”.

Thus motivated, and also provoked by recent experimental (Laubereau and Iglev, 2013) and satellite-borne measurements (Feldman *et al.*, 2015; Rentsch, 2019) which pointed consistently to a rather low climate sensitivity, we make here another attempt to quantify the respective shares of anthropogenic and heliogenic climate drivers. Specifically, we resume the long tradition of correlating terrestrial temperature data with certain proxies of solar activity, as pioneered by Reid (1987) for the sunspot numbers, by Friis-Christensen and Lassen (1991); Solheim, Stordahl and Humlum (2015) for the solar cycle length, and by Cliver, Boriakoff and Feynman (1998); Mufti and Shah (2011) for the geomagnetic aa-index (Mayaud, 1972). Our work builds strongly on the two latter papers, which - based on data ending in 1990 and 2007, respectively - had found empirical correlation coefficients between the aa-index and temperature variations of up to 0.95. Notwithstanding some doubts regarding their statistical validity (Love *et al.*, 2011), such remarkably high correlations might rise the provocative question of whether any sort of greenhouse effect *is still needed at all* to explain the (undisputed) global warming over the last one and a half century. More recently, however, any prospects for such a *reversed* simplification were dimmed by the fact that the latest decline of the aa-index was not accompanied by a corresponding drop of temperature. By contrast, the latter remained rather constant during the first one and a half decades of the 21st century (the “hiatus”), and even increased with the recent strong El Niño events.

This paper aims at supplementing the previous work of Cliver, Boriakoff and Feynman (1998); Pulkkinen *et al.* (2001); Mufti and Shah (2011); Zhrebtsov *et al.* (2019) by taking seriously into account both observations: the nearly perfect correlation of solar activity with temperature over about 150 years, and the notable divergence between those quantities during the last two decades. Using a multiple regression analysis, quite similar to that of Soon, Posmentier and Baliunas (1996), but with the time series of the aa-index as the second independent variable (in addition to the logarithm of CO₂ concentration), we will show that the temperature variation since the middle of the 19th century can be reproduced with an (adjusted) R^2 value around 87 per cent. Such a goodness-of-fit is achieved for specific combinations of the weights of the aa-index and of CO₂ that form a nearly linear function in their two-dimensional parameter space. Best results are obtained for a climate sensitivity in the range between 0.6 K-1.6 K (per $2\times$ CO₂), with a delicate dependence on whether the latest data are included or not. Derived from empirical variations on the (multi-)decadal time scale, this climate sensitivity should be interpreted as a transient climate response (TCR), rather than an ECS. Our range corresponds well with that of Lewis and Curry (2018), 0.8 K-1.3 K, but is appreciably lower than the “official” 1.0 K-2.5 K range (Knutti *et al.*, 2017). The lower edge of our estimation will be plausibilized by recent experimental (Laubereau and Iglev, 2013) and satellite-borne measurements (Feldman *et al.*, 2015; Rentsch, 2019). It is also quite close, al-

though still higher, than the particularly low estimate of less than 0.44 K, as advocated by Soon, Conolly and Conolly (2015) after comparing exclusively rural temperature data in the Northern hemisphere with the TSI. The upper edge, in turn, is not far from the spectroscopy-based estimation by Wijngaarden and Happer (2020).

With the complementary share of the Sun for global warming thus reaching values between 30 and 70 per cent, any climate forecast will require a descent prediction of solar activity. This leads us into yet another controversial playing field, viz, the predictability of the solar dynamo. While the existence of the short-term Schwabe/Hale cycles is a truism in the solar physics community, the existence and/or stability of the mid-term Gleissberg and Suess-de Vries cycles are already controversially discussed, and there is even more uncertainty about long-term variations such as the Eddy and Hallstatt “cycles”, which are closely related to the sequence of Bond events (Bond *et al.*, 2001).

In a series of recent papers (Stefani *et al.*, 2016, 2017, 2018; Stefani, Giesecke and Weier, 2019; Stefani *et al.*, 2020a,b; Stefani, Stepanov and Weier, 2020), we have tried to develop a self-consistent explanation of those short-, medium- and long-term solar cycles in terms of synchronization by planetary motions. According to our present understanding, the surprisingly phase-stable 22.14-year Hale cycle (Vos *et al.*, 2004; Stefani *et al.*, 2020b) results from parametric resonance of a conventional $\alpha - \Omega$ dynamo with an oscillatory part of the helical turbulence parameter α that is thought to be synchronized by the 11.07-year spring-tide periodicity of the three tidally dominant planets Venus, Earth, and Jupiter (Stefani *et al.*, 2016, 2017, 2018; Stefani, Giesecke and Weier, 2019). The medium-term Suess-de Vries cycle (specified to 193 years in our model) emerges then as a *beat period* between the basic 22.14-year Hale cycle and some (yet not well understood) spin-orbit coupling connected with the motion of the Sun around the barycenter of the solar system that is governed by the 19.86-year synodes of Jupiter and Saturn (Stefani *et al.*, 2020a; Stefani, Stepanov and Weier, 2020). Closely related to this, some Gleissberg-type cycles appear as nonlinear beat effects and/or from perturbations of Sun’s orbital motion from other synodes of the Jovian planets. Finally, the long-term variations on the millennial time-scale (Bond events) arise as chaotic transitions between regular and irregular episodes of the solar dynamo (Stefani, Stepanov and Weier, 2020), in close analogy with the supermodulation concept introduced by Weiss and Tobias (2016).

Being well aware of the conjectural nature of this synchronized solar dynamo model, we nevertheless dare to make a cautious prediction of the aa-index for the next 130 years, based on some simple 3-frequency fits to the aa-index data over the last 170 years. While our choice for three frequencies is motivated by the dominance of one Suess-de Vries and two Gleissberg-type cycles, we employ different versions of fixing or relaxing their frequencies, which leads to a certain variety of forecasts. A common feature of all of them is, however, a noticeable decline of solar activity until 2100, and a recovery in the 22nd century. Those predictions for

the aa-index are then combined with three different scenarios of CO₂ increase, including an unfettered annual increase by 2.5 ppm and two further scenarios based on hypothetical decarbonization schemes. The 3 × 3 models thus obtained are then blended with the different combinations of weights for the aa-index and CO₂ as derived before in the regression analysis. For the “hottest” scenario we predict an additional temperature increase until 2100 of less than 1 K, while all other combinations lead to less warming, partly even to some imminent cooling, followed by a rather flat behaviour in which decreasing solar activity and a mildly increasing trend from CO₂ compensate each other to a large extent.

2. Multiple regression analysis

In this section, we perform a multiple (or better: double) regression analysis of the temperature data (dependent data) on the geomagnetic aa-index and the logarithm of the CO₂ (independent data). We do this in an intuitive and easily reproducible way by showing the *fraction of variance unexplained* (FVU), i.e. the ratio of the residual sum of squares to the total sum of squares, whose minimum is then identified. From those FVU's we will derive the corresponding R^2 value, both in its usual and in its adjusted variant. Let us start, however, with a description of our data base.

2.1. Data

While reliable CO₂ data are available for quite a long time, we decided to restrict our data base to the time from the middle of the 19th century, for which both temperature data and the aa-index are readily available.

2.1.1. Temperature data

There are quite a number of different temperature series which might be considered as basis for regression analysis. In order to make contact with the work of Mufti and Shah (2011), we decided to use the Hadley Centre Sea Surface Temperature (HadSST) data set in its updated version HadSST.4.0.0.0, available from www.metoffice.gov.uk, which provides us the sea surface temperature anomaly from 1850 until 2018, relative to the 1961–1990 average (Kennedy *et al.*, 2019). Actually, these data are not gravely different from the combined sea/land surface temperature (HadCRUT), apart from some slight but systematic divergence during the last two decades. At this point, our preference for HadSST is also supported by their better agreement with the UAH satellite data (starting only in 1978) with their significantly broader spatial coverage.

The HadSST data are shown as open circles in Fig. 1a, together with two exemplary centered moving averages with windows 11 years (full line) and 23 years (dashed line), which we will frequently refer to in this paper. These curves show the typical temporal structure comprising a slow decay between 1850 and 1905, a rather steep rise between 1905 until 1940, again a mild decay until 1970, followed by a steep increase until 1998. As for the last two decades, we first see the “hiatus” between 1999 and 2014, being then overwhelmed

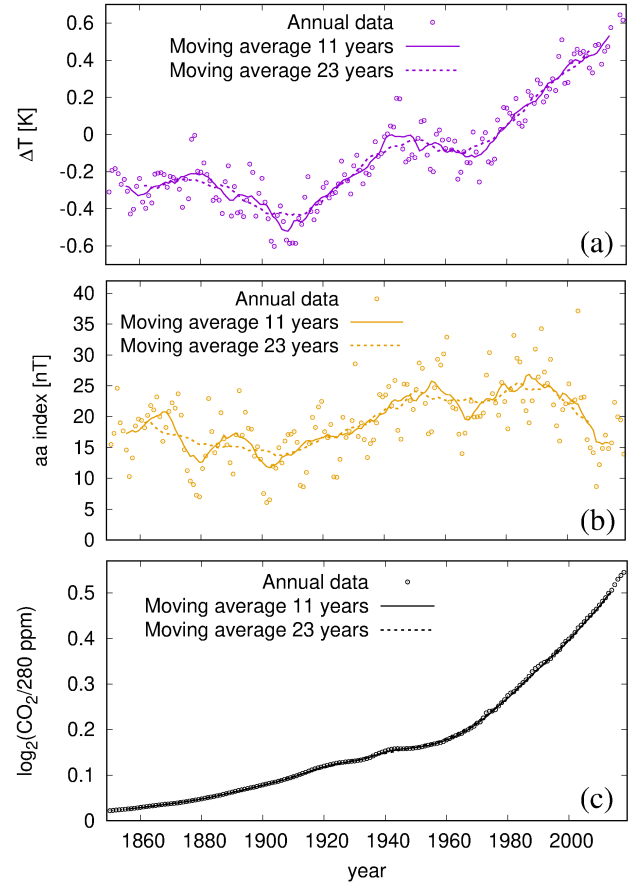


Figure 1: Data of the HadSST sea surface temperature anomaly ΔT (a), the aa-index (b), and \log_2 of the ratio of the CO₂ concentration to the reference value of 280 ppm (c). The annual data between 1850–2018 are complemented by centered moving averages with windows 11 years and 23 years, as also utilized by Mufti and Shah (2011). The sources of the data are described in the text.

by the recent strong El Niño events. We will come back to those latest years further below.

2.1.2. aa-index data

The aa-index measures the amplitude of global geomagnetic activity during 3-hour intervals at two antipodal magnetic observatories, normalized to geomagnetic latitude $\pm 50^\circ$ (Mayaud, 1972). Inspired by the work of Cliver, Boriakoff and Feynman (1998) and Mufti and Shah (2011) who pointed out the remarkable correlation of up to 0.95 between (time averaged) temperature anomalies and the geomagnetic aa-index, we will use the latter data as a proxy for solar activity. A viable alternative would have been to use sunspot data, or various versions of the TSI, as exemplified by Soon, Conolly and Conolly (2015). Given, on one side, their generally high correlation with sunspots numbers (Cliver, Boriakoff and Bounar, 1998), and, on the other side, their high reliability based on precise measurement down to 1844 (which avoids some ambiguities concerning the correct variability of the TSI (Soon, Conolly and Conolly, 2015; Connolly *et al.*, 2021)), we focus here exclusively on the aa-index, leaving

multiple regressions analyses with other solar data to future work.

The bulk of the aa-index data, between 1868-2010, was obtained from ftp.ngdc.noaa.gov. As in Mufti and Shah (2011), the early segment between 1844 and 1867 was taken from Nevanlinna and Kataja (1993). The latest segment, between 2011 and 2018, was obtained from www.geomag.bgs.ac.uk. All these aa-index data were annually averaged. Together with their 11-year and 23-year moving averages, the annual aa data are shown in Fig 1b. Already by visual inspection, between 1850 and 1990 we observe a remarkable similarity of their shape with that of temperature, while after 1995 the aa-index steeply declines, whereas the temperature continues to increase. We will have more to say on that divergence further below.

2.1.3. CO₂ data

The CO₂ concentration data until 2014 were obtained from iac.ethz.ch/CMIP6/. The four additional data points from 2015 and 2018 were taken from the website www.co2.earth. Together with their 11-year and 23-year moving averages the logarithm of those data is shown on Fig. 1c.

2.2. Are we dealing with the most relevant data?

After having presented the data that actually will be used in the remainder of this paper, we make a short break to consider whether these are indeed the most relevant data. Our reliance on the aa-index might indeed be questioned, as other studies (Vahrenholt and Lüning, 2020) have claimed a strong temperature dependence on ocean-atmosphere variations, such as the Pacific Decadal Oscillation (PDO) (Mantua and Hare, 2002) and the Atlantic Multidecadal Oscillation (AMO) (Wyatt, Kravtsov and Tsonis, 2012), with their similar time structures governed by a sort of 60-70-year “cyclicity”. On the other hand, there is also evidence for direct correlations of the aa-index with regional features, such as the Northern Annular Mode (NAM) (Roy *et al.*, 2016). In order to make contact with those possible links, in Fig. 2 we show exemplarily the 23-year averages of the AMO and the PDO data, together with the previously shown aa-index (appropriately shifted and scaled) and ΔT . It is clearly seen that the aa-index and ΔT have a particularly parallel behaviour until 1990, say. There is also some similarity with AMO, while PDO has a different time dependence.

In Table 1 we quantify those relationships in terms of the empirical correlation coefficients r for different data combinations. We do so for different end points of the time interval, namely 2008, 2003 and 1998 (note that these are the centered points of the last moving average interval, into which the annual data from up to 11 years later are included). Our first observation is that both the correlations of CO₂ and of the aa-index with ΔT have similar r -values in the order of 0.9, which is a first indication for their comparable influences. However, there are some subtleties to discern: the correlation for CO₂ acquires its highest value ($r = 0.916$) for the full time interval, and decreases slightly to 0.869 when the time interval is shortened by 10 years. By contrast, the correlation of aa-index with ΔT has only a value $r = 0.8$

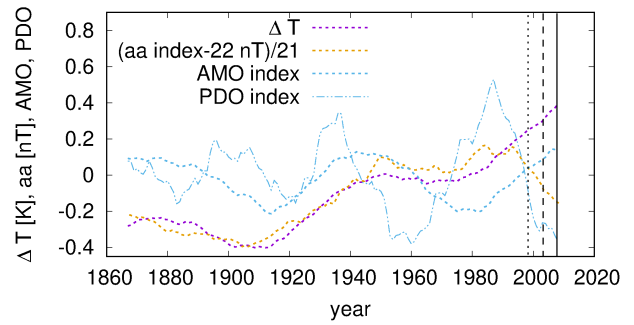


Figure 2: Comparison between the centered moving averages over 23 years of the four data sets ΔT , aa-index, AMO-index and PDO-index. Note the remarkable parallelism of ΔT and aa-index until 1990, and the divergence thereafter. The AMO-index has also some similarity with ΔT , while the PDO index is significantly different.

for the full interval, but grows to 0.95 for the restricted interval. This latter result confirms that of Mufti and Shah (2011) obtained for a similar period, and by Cliver, Boriakoff and Feynman (1998) for a still shorter interval. Given the visual similarity of AMO and ΔT in Fig. 2, their correlation is surprisingly small, but would increase if the overall upward trend of ΔT were subtracted. The PDO seems to show no relevant correlation with ΔT .

Table 1

Empirical correlation coefficients r between different data sets, each of which represents a centered moving average over 23 years. Note the large values for the correlation both between CO₂ and the aa-index with ΔT , compared to weak or barely existing correlations of the AMO- and PDO-index with ΔT .

Correlated data	1867-2008	1867-2003	1867-1998
CO ₂ with ΔT	0.916	0.894	0.869
aa with ΔT	0.806	0.900	0.950
AMO with ΔT	0.260	0.164	0.106
aa with AMO	-0.015	-0.013	-0.028
PDO with ΔT	-0.131	-0.001	0.126
aa with PDO	0.050	0.049	0.074

In Fig. 3 we show some further correlation dependencies, this time on the time shift δt between the two respective data, which possibly could give a clue about intrinsic delay effects. One curve shows the correlation between the aa-index and the AMO index, whereby the aa-index at earlier times is correlated with AMO at later times. While the correlation is not large, we see at least a clear maximum at $\delta t = 11$ years, as if the AMO-index lagged behind the aa-index by this delay time. The second curve shows the corresponding relationship between ΔT and AMO, with the correlation reaching a maximum of 0.3 at $\delta t = 6$ years. While this looks like a sort of inverted causality (AMO lags behind ΔT) it could simply mean that ΔT is indeed governed by the aa-index, which also determines the AMO-index at later times.

We also show the corresponding curves for aa-index and

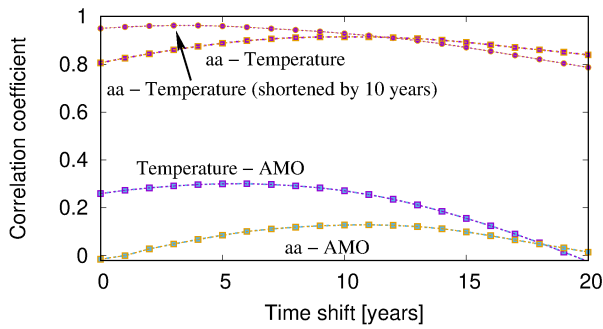


Figure 3: Correlations between various data, each representing a 23-years centered moving average, in dependence on the time shift δt between them. In each case, the first item indicates the earlier data set, the second the later one. The aa- ΔT correlation starts at the value $r = 0.8$ for $\delta t = 0$ and reaches a maximum of $r = 0.915$ for $\delta t = 10$ years. While this might insinuate a 10-years causal time shift between aa-index and ΔT , it is more likely connected with the canceling effect of the latest decade with its poor correlation. In the second curve, for which we have completely omitted the last 10 years of both data, we get $r = 0.95$ at $\delta t = 0$, increasing to a maximum of $r = 0.962$ at $\delta t = 3$ years. Compared to those large r -values, the correlation of ΔT and AMO is much smaller, viz 0.3 at $\delta t = 6$ years (AMO lagging behind temperature). Still smaller is the correlation of aa-index and AMO, with a maximum of $r = 0.129$ for $\delta t = 11$ years.

ΔT , in the two versions for the full time interval and the 10-year shortened one. For the full interval, r starts at the value 0.8 for $\delta t = 0$, but reaches a maximum of 0.915 for $\delta t = 10$ years. While on face value this seems to indicate a 10-years lag between the aa-index and ΔT , it is more likely connected with the implied cancellation of the last 10 years during which the aa-index was decreasing. In order to test this, in the second curve we have omitted the last 10 years of both data completely. Here we find an $r = 0.95$ at $\delta t = 0$, which still increases to a maximum of $r = 0.962$ at $\delta t = 3$ yr. This sounds indeed like a reasonable time delay between cause (aa-index) and effect (ΔT).

2.3. Regression

After those preliminaries, we start now with the multiple regression analysis. For that purpose, we model the temperature data using the ansatz

$$\Delta T^{\text{model}} = w_{\text{aa}} \cdot \text{aa} + w_{\text{CO}_2} \cdot \log_2(\text{CO}_2/280 \text{ ppm})$$

with the respective weights w_{aa} and w_{CO_2} for solar and CO_2 forcing, and compare them with the measured data ΔT^{meas} . This procedure is very similar to that of Soon, Posmentier and Baliunas (1996) who had used though, instead of aa, the length of the sunspot cycle, the averaged sunspot number, and a more complicated composite as proxies of solar irradiance. While Soon, Posmentier and Baliunas (1996) translate all these proxies into some percentage of TSI variation (fixing their “stretching factor” by the best fit of modeled and observed temperature history), we stick here to the somewhat weird unit K/nT for w_{aa} , without specifying in detail the

physical mechanism(s) underlying the solar-climate connection. In case of a dominant Svensmark effect, say, this unit would indeed have an intuitive physical meaning, whereas in case of a dominant UV radiation impact on the ozone layer (plus subsequent coupling of stratosphere and troposphere), it would just represent a very indirect, co-responding proxy.

One of the non-trivial questions to address beforehand is which time average should be used. Evidently, the structures of temporal fluctuation of the three data are quite different. As for the independent data, the CO_2 curve is the smoothest one, so the results of any regression will be widely independent on the widths of the averaging window. Much more fluctuating is the aa-index, with its dominant 11-year periodicity which had been taken into account, though in different ways, by Cliver, Boriakoff and Feynman (1998) and Mufti and Shah (2011). Cliver, Boriakoff and Feynman (1998) have been working both with a decadal average and the so-called aa-baseline (aa_{min}), i.e. the minimum value which generally occurs within one year following the sunspot minima. The empirical correlation coefficient of $r = 0.95$ between aa_{min} and the 11-year average temperature turned out to be even better than that between two decadal averages ($r = 0.9$). Mufti and Shah (2011), in turn, worked with 11-year and 23-year averages, which will also serve as a first guidance for our study, though later we will consider the dependence on the widths of the averaging windows in a more quantitative manner.

The dependent variable, i.e. ΔT , is also characterized by significant fluctuations, although not with the dominant 11-year periodicity of the aa-index whose climatic impact is thought to be smoothed out by the large thermal inertia of the oceans. By contrast, ΔT is strongly influenced by short-term variations due to the El Niño-Southern Oscillation (ENSO) and volcanism, which had been considered in the multiple regression analysis of Lean and Rind (2008). Our deliberate neglect of those short-term variations, and the focus on (multi-)decadal variations, thus requires some averaging on the decadal time scale.

In addition to that distinction between different averaging windows, we will also consider three cases with different end-years of the utilized data. In the first case, we take into account all data until 2018. As evident from Fig. 1, it is in particular the last decade which shows the strongest discrepancy between the decreasing aa-index and the partly stagnant (“hiatus”), partly increasing temperature (in particular during the last El Niño dominated years). Hence, in order to assess the specifics of this divergence between the two data, and to compare them with the high correlations found by Cliver, Boriakoff and Feynman (1998) and Mufti and Shah (2011), we will also consider two shortened periods with end years 2013 and 2008, respectively.

Let us start, however, with the full data ending in 2018. For the two moving average windows (abbreviated henceforth as “MAW”) of 11 years and 23 years, Figs. 4a and 4b show the *fraction of variance unexplained* (FVU), i.e. the ratio of the residual sum of squares to the total sum of squares, in dependence on the respective weights of the aa-

index (w_{aa} , on the abscissa) and the logarithm of CO_2 (w_{CO_2} , on the ordinate axis). The latter value provides us immediately with a sort of instantaneous climate sensitivity of the TCR type. The minimum $\text{FVU}_{\min} = 0.107$ is obtained for the weights' combination $w_{aa} = 0.011 \text{ K/nT}$ and $w_{\text{CO}_2} = 1.72 \text{ K}$ in case of $\text{MAW} = 11$ years, and $\text{FVU}_{\min} = 0.102$ is obtained for $w_{aa} = 0.0162 \text{ K/nT}$ and $w_{\text{CO}_2} = 1.54 \text{ K}$ in case of $\text{MAW} = 23$ years. From the ellipse-shaped contour plots of FVU we see that those minima reflect a dominating influence of CO_2 over the aa-index. The two red curves in Fig. 6c show now the corresponding temperature reconstructions based on those optimized values of w_{aa} and w_{CO_2} , for $\text{MAW} = 11$ years (full line) and for $\text{MAW} = 23$ years (dashed line). For both lines we obtain a reasonable fit of the general upward trend of ΔT , but a poor reconstruction of its oscillatory features. This clearly corresponds to the comparable high value of w_{CO_2} compared to that of w_{aa} . Any putative higher share of w_{aa} would lead to a drastic decrease of the reconstructed ΔT for the last two decades, resulting in forbiddingly large FVU values when compared with the relatively high observed ΔT in this late period.

This brings us to the question of what happens if we exclude the latest “hot” 5 years (with their strong El Niño influence), thus restricting the date until 2013 only. The corresponding results are shown in Fig. 5. Obviously, the optimal weights' combination now shifts away from CO_2 to aa, with values $w_{aa} = 0.0145 \text{ K/nT}$ and $w_{\text{CO}_2} = 1.56 \text{ K}$ for $\text{MAW} = 11$ years and $w_{aa} = 0.0232 \text{ K/nT}$ and $w_{\text{CO}_2} = 1.21 \text{ K}$ for $\text{MAW} = 23$ years. Evidently, the resulting (green) temperature reconstruction curves in Fig. 5c appear now more oscillatory.

In Fig. 6 we show the corresponding plots for the case that we use the end year 2008, which basically corresponds to the database of Mufti and Shah (2011) (2007 in their case). Evidently, the regression for this shortened segment leads to a significantly stronger weight for the aa-index. The minimum FVU is than obtained at $w_{aa} = 0.0190 \text{ K/nT}$ and $w_{\text{CO}_2} = 1.33 \text{ K}$ for $\text{MAW} = 11$ years, and at $w_{aa} = 0.0305 \text{ K/nT}$ and $w_{\text{CO}_2} = 0.80 \text{ K}$ for $\text{MAW} = 23$ years. Due to the dominance of w_{aa} the (blue) reconstruction curves in Fig. 6c (in particular that for $\text{MAW} = 23$ years) show now a significant oscillatory behaviour.

While those three examples provide a first illustration of how sensible the solution of the regression reacts on the choice of the end year, and the widths of the MAW, the latter dependence will now be studied in more detail. For that purpose, we analyze first the *coefficient of determination* R^2 , which is related to the previously used FVU according to $R^2 = 1 - \text{FVU}$. The corresponding dashed curves in Fig. 7a have a rather universal shape, starting from values of 0.78...0.84 for $\text{MAW} = 3$ years to around 0.94 for $\text{MAW} = 39$ years. The monotonic increase of R^2 , which at first glance might suggest the use of high values of MAW, should be treated with caution. The reason is that a significant share of this increase is just due to the increasing ratio of explanatory terms p (in our case two: w_{aa} and w_{CO_2}) to the “honest” number of data points n . The latter is not

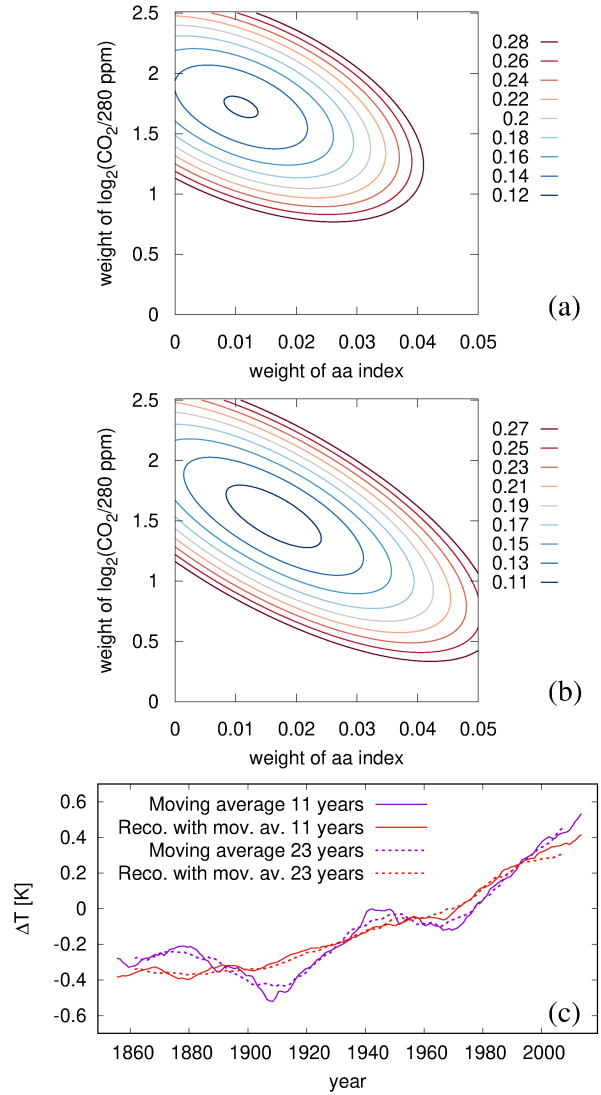


Figure 4: Regression analysis for the full data (with end year 2018). (a) FVU in dependence on w_{aa} and w_{CO_2} for $\text{MAW} = 11$ years, with $\text{FVU}_{\min} = 0.107$ reached for $w_{aa} = 0.011 \text{ K/nT}$ and $w_{\text{CO}_2} = 1.72 \text{ K}$. (b) The same for $\text{MAW} = 23$ years, with $\text{FVU}_{\min} = 0.102$ reached for $w_{aa} = 0.0162 \text{ K/nT}$ and $w_{\text{CO}_2} = 1.54 \text{ K}$. (c) 11-year and 23-year moving averages for the original ΔT (purple) and for the reconstructed ΔT (red) when using the optimized values of w_{aa} and w_{CO_2} from (a) and (b).

identical to the number of considered years, N_y , but - due to the moving average - approximately equal to N_y/MAW (better estimates, using the lag-one auto-correlation r^1 (Love et al., 2011), might still be worthwhile). To correct for this effect, we use the so-called adjusted R^2 , which is, in general, $\bar{R}^2 = 1 - \text{FVU} \times (n - 1)/(n - p - 1)$, hence in our special case $\bar{R}^2 = 1 - \text{FVU} \times (N_y/\text{MAW} - 1)/(N_y/\text{MAW} - 3)$. This adjusted \bar{R}^2 , as a much more telling coefficient of determination than R^2 , is shown with full lines in Fig. 7a. The monotonic increase still seen for R^2 gives now way to a more structured curve. For the green (data until 2013) and the blue curve (data until 2008) we observe a local (if shallow)

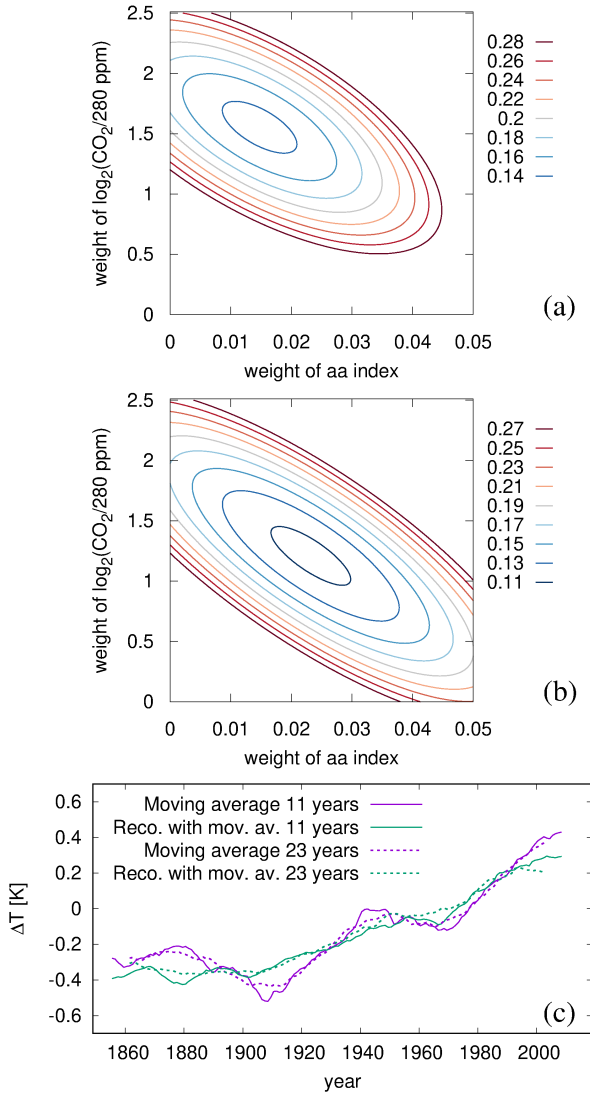


Figure 5: Regression analysis for the reduced data (end year 2013). (a) FVU in dependence on w_{aa} and w_{CO_2} for MAW = 11 years, with $\text{FVU}_{\min} = 0.134$ reached for $w_{aa} = 0.0145 \text{ K/nT}$ and $w_{\text{CO}_2} = 1.56 \text{ K}$. (b) The same for MAW = 23 years, with $\text{FVU}_{\min} = 0.105$ reached for $w_{aa} = 0.0232 \text{ K/nT}$ and $w_{\text{CO}_2} = 1.21 \text{ K}$. (c) 11-year and 23-year moving averages for the original ΔT (purple) and for the reconstructed ΔT (red) when using the optimized values of w_{aa} and w_{CO_2} from (a) and (b).

maximum around MAW = 25 years. The red curve (data until 2018) has a very flat plateau between MAW = 11 and MAW = 27 years, with an extremely shallow maximum at MAW = 25 years. We consider those local maxima around MAW = 25 years (MAW = 27 years for the blue curve) as a sort of best fits. Although \bar{R}^2 still rises slightly for the highest MAW values, the corresponding number of explained variables becomes then too small to allow for a decent reconstruction of the structure of the ΔT curve.

The corresponding dependencies for w_{aa} and w_{CO_2} are shown in Fig. 7b and 7c, respectively. Fig. 7d depicts the same solutions in the two-dimensional parameter space. In this representation, all three curves (red, green and blue)

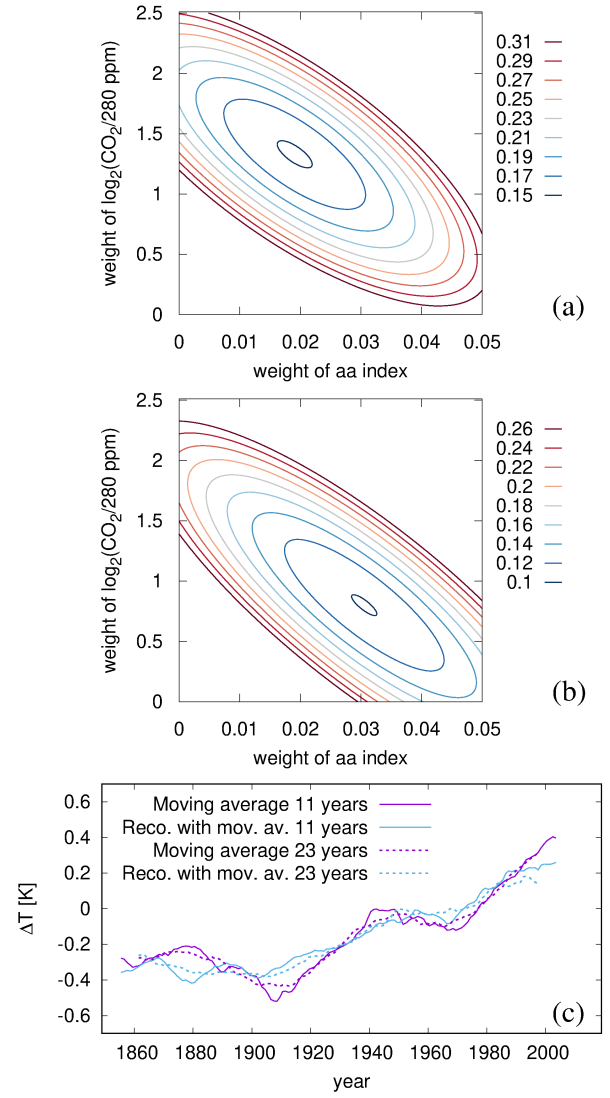


Figure 6: Regression analysis for the reduced data (end year 2008). (a) FVU in dependence on w_{aa} and w_{CO_2} for MAW = 11 years, with $\text{FVU}_{\min} = 0.149$ reached for $w_{aa} = 0.019 \text{ K/nT}$ and $w_{\text{CO}_2} = 1.33 \text{ K}$. (b) The same for MAW = 23 years, with $\text{FVU}_{\min} = 0.099$ reached for $w_{aa} = 0.0305 \text{ K/nT}$ and $w_{\text{CO}_2} = 0.80 \text{ K}$. (c) 11-year and 23-year moving averages for the original ΔT (purple) and for the reconstructed ΔT (red) when using the optimized values of w_{aa} and w_{CO_2} from (a) and (b).

form a sort of common, weakly bent line which appears to connect the extremal values of $w_{\text{CO}_2} \approx 1.9 \text{ K}$ on the ordinate axis and $w_{aa} \approx 0.04 \text{ K/nT}$ on the abscissa. This common line is just a reflection of the ellipsoidal shape of the FVU as shown in Figs. 3-5 which, in turn, just reflects the significant ill-posedness of the underlying inverse problem. To put it differently: due to the high correlation coefficients of ΔT both with CO_2 as well as with the aa-index, the separate shares of the two ingredients are very hard to determine.

However questionable our fixation on the shallow maxima at MAW ≈ 25 years might ever be: Fig. 7 also proves that any alternative choice of a higher MAW would not change the final solution drastically. In either case, both w_{aa} and

w_{CO_2} converge to a close-by value. Much more decisive is the distinction between the differently colored curves: for w_{CO_2} , they give us results somewhere between 0.6 K and 1.6 K (in the latter case we take into account the particular flatness of the maximum, which in reality might also lay at slightly lower values of MAW).

Actually, this is again a frustratingly wide range of values. As said, it reflects the ill-posedness of the underlying inverse problem, whose non-uniqueness leads also to a high sensitivity on neglected factors, such as ENSO, AMO, PDO, volcanic aerosols. At any rate, the temperature development during the next decade will be key: if it continues to grow we will end up at the higher end of the w_{CO_2} range. In case of some imminent drop it will point to lower values of w_{CO_2} .

In Fig. 8 we show all three temperature reconstructions with the optimal combinations of w_{aa} and w_{CO_2} taken from Fig. 7, together with the original ΔT data, averaged over 25 years. The dashed segments of the green and blue curves correspond to the later time segments which were deliberately omitted in the corresponding regression analysis. As expected, they exhibit an increasing divergence from the original ΔT data. On the other hand, from the red via the green to the blue curve we also observe an improved reconstruction of the oscillatory behaviour of ΔT . This is the crux of our problem: the better the reconstruction for the years until 1995, say, the larger is the deviation for the latest two decades. We will need approximately one decade of more data to being able to identify the best solution. For the green or blue lines to be valid, a significant temperature drop in the nearest future will be unavoidable.

2.4. Some plausibility checks and comparisons

Before entering the field of predictions, we would like to check the plausibility of the obtained estimates, in particular those at the lower end of the range. For that purpose we will shortly discuss the results of three papers which are based on experimental and satellite-borne measurements.

Combining measurements at optically thick samples of CO_2 with a 5-layer numerical model for the greenhouse effect, Laubereau and Iglev (2013) had derived a temperature increase of 0.26 K for the 290 ppm to 385 ppm increase between 1880 and 2010, which results in a climate sensitivity of 0.636 K (per $2\times\text{CO}_2$)

Feldman *et al.* (2015) had published results from two clear-sky surface radiative forcing measurements with the Atmospheric Emitted Radiance Interferometer (AERI) between 2000 and 2010, when the CO_2 concentration increased (according to their estimate) by 22 ppm. They observed an increase of 0.2 W/m^2 during this decade, which amounts to 2.4 W/m^2 (per $2\times\text{CO}_2$). With the usual zero-feedback sensitivity parameter of 3.7 $\text{K}/(\text{W}/\text{m}^2)$, this translates into 0.65 K (per $2\times\text{CO}_2$). If we were to use the modified value of 3.2 $\text{K}/(\text{W}/\text{m}^2)$ (which allows for variations with latitude (Soden and Held, 2006)), we get 0.75 K.

Later on, Rentsch (2019) found a similar result by analyzing outgoing radiation under night-time, cloud-clear conditions. The CO_2 rise from 373 ppm to 410 ppm led to a

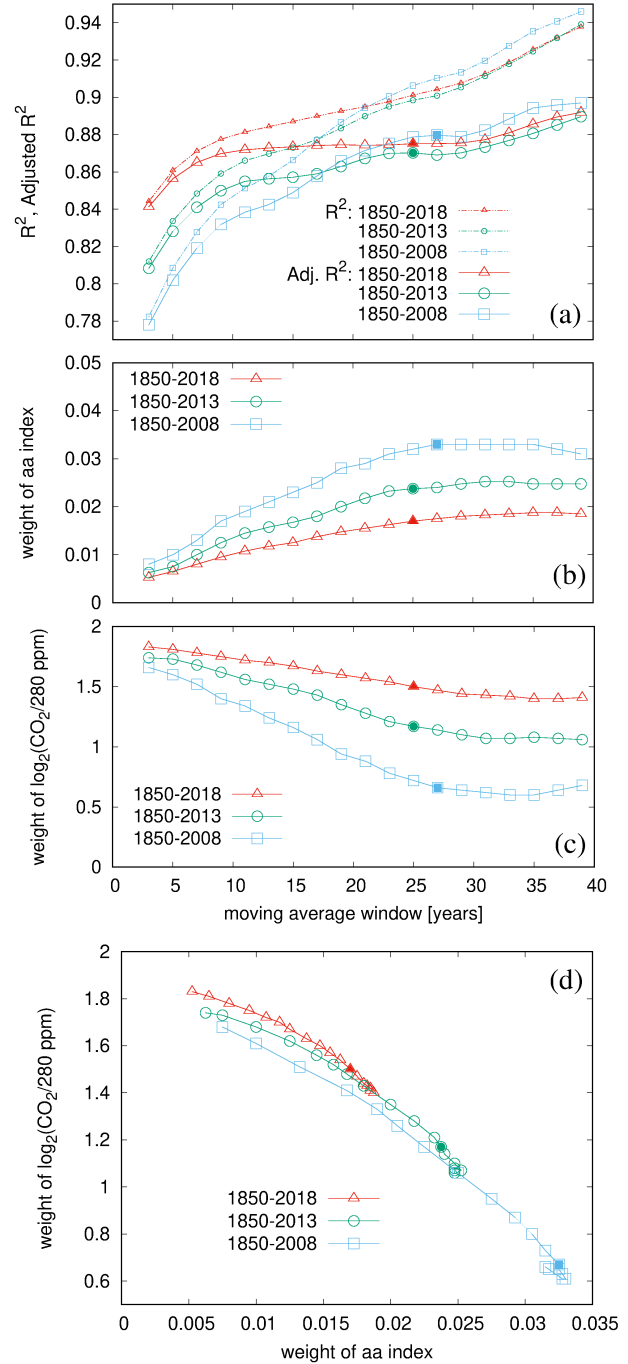


Figure 7: Results of the regression in dependence on the width of the moving average window (MAW). (a) R^2 and its adjusted version \bar{R}^2 , each for the three time intervals ending in 1818, 2013, 2008. The (shallow) local maxima of \bar{R}^2 around MAW = 25 years are indicated by full symbols. (b) w_{aa} in dependence on MAW. The full symbols are the values corresponding to the local maxima in (a). (c) same as (b), but for w_{CO_2} . (d) Regression result in the two-dimensional parameter space of w_{aa} and w_{CO_2} . Note the universal shape of the solution given a slightly bent, but nearly linear function connecting the extremal values $w_{\text{CO}_2} \approx 1.9 \text{ K}$ on the ordinate axis and $w_{\text{aa}} \approx 0.04 \text{ K/nT}$ on the abscissa.

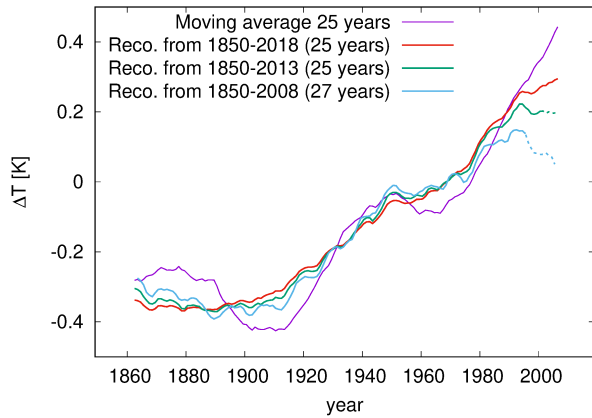


Figure 8: Original ΔT data, averaged over 25 years, and reconstructions based on the optimal combinations of w_{aa} and w_{CO_2} from Fig. 7. The dashed segments of the green and blue curves indicate those time intervals that did not enter in the respective regressions. From the red over green to blue curve, we see an ever improving reconstruction of the oscillatory behaviour, and an ever increasing divergence with the observed data at later years.

forcing of 0.358 W/m^2 , corresponding to 2.63 W/m^2 (per $2 \times CO_2$), i.e. to 0.71 K (with $3.7 \text{ K/(W/m}^2)$) or 0.82 K (with $3.2 \text{ K/(W/m}^2)$), in nearly perfect agreement with Feldman *et al.* (2015).

These three papers are widely consistent among each other, giving sensitivities in the range between 0.64 K and 0.82 K , which is close to the lower edge of our estimate. We also note that this end of our regression, which corresponds to approximately 70 per cent “for the sun”, is similar to the 50–69 per cent range as once found by Scafetta and West (2007, 2008).

This said, we should also note that Wijngaarden and Happer (2020) have found the much higher value of 1.4 K value (at fixed absolute humidity) which would fit to our upper limit of 1.6 K value which is, in turn, significantly lower than their value $2.2\text{--}2.3 \text{ K}$, as inferred for fixed relative humidity.

The range of our estimates is slightly sharper as the range 0.4 K to 2.5 K of Soon, Conolly and Conolly (2015) (with the high value deemed unrealistic by the authors), and slightly wider than the 0.8 K – 1.3 K range of Lewis and Curry (2018), but in either case quite consistent with those estimations.

3. Predictions

In the preceding section we have derived a certain plausible range of combinations of the respective weights of the aa-index and the logarithm of CO_2 by means of regression analysis of data from the past 170 years. In the following we will leave the realm of solid, data-based science and enter the somewhat “magic” realm of predictions. Given all the underlying uncertainties concerning the future time dependence of the aa-index, of CO_2 , and of further climate factors such as AMO, PDO, ENSO, volcanism etc., any forecast has to be taken with more than one grain of salt. This said, we

will at least do some parameter studies, by allowing the unknown time series of the aa-index and CO_2 , and their respective weights, to vary in some reasonable range. Let us start with the aa-index.

3.1. Predicting the solar dynamo

This subsection is definitely the most speculative one of this paper as it is concerned with forecasts of the aa-index for the next 130 years. There is no doubt that the aa-index is strongly correlated with the sunspot number (SSN), with typical correlation coefficients of around $r = 0.96$ when averaged over one cycle Cliver, Boriakoff and Bounar (1998). Neither is there any doubt that the SSN and the aa-index are both governed (though in a non-trivial manner) by the solar dynamo. So any prediction of the aa-index boils down to a prediction of the solar dynamo which many researchers believe to be impossible, at least beyond the horizon of the very next cycle for which reasonable (though not undisputed) “precursor methods” exist (Svalgaard, Cliver and Kamide, 2005; Petrovay, 2010).

In order to justify our audacious forecast for the aa-index, we have to make a little diversion on the solar dynamo and its short-, medium- and long-term cycles. The reader should be warned, though, that our arguments do not reflect the mainstream of solar dynamo theory. We think nevertheless that the last years have brought about sufficient empirical evidence that justifies at least a cautious try.

Let us start with some recent evidence concerning the phase stability of the Schwabe cycle, a matter that was first discussed by Dicke (1978). In Stefani *et al.* (2020b) we have reviewed the pertinent results derived from algae data in the early Holocene (Vos *et al.*, 2004) and from sunspot and *aurorae borealis* observations, combined with ^{14}C and ^{10}Be data, from the last centuries. Without going into the details it was shown that the Schwabe cycle is very likely phase-stable at least over some centuries, with a period between 11.04 years and 11.07 years. While certain nonlinear self-synchronization mechanisms of the solar dynamo cannot be completely ruled out as an explanation (Hoyng, 1996), the external synchronization by the 11.07-years periodic spring tides of the (tidally dominant) Venus–Earth–Jupiter system provides a suspiciously compelling alternative. Based on previous observations and ideas of Hung (2007); Wilson (2008); Scafetta (2012); Wilson (2013); Okhlopov (2016), we have corroborated a model (Weber *et al.*, 2015; Stefani *et al.*, 2016, 2017, 2018; Stefani, Giesecke and Weier, 2019) in which the weak tidal forces of Venus, Earth and Jupiter serve only as an external trigger for synchronizing (via parametric resonance) the intrinsic helicity oscillations of the kink-type Tayler instability in the tachocline region. The arising 11.07-yr period of the helicity parameter α ultimately leads to the 22.14 year period of the Hale cycle.

Building on this phase coherence of the Hale cycle, later (Stefani *et al.*, 2020a; Stefani, Stepanov and Weier, 2020) we exploited ideas of Wilson (2013); Solheim (2013) to explain the mid-term Suess-de Vries cycle as a beat period between the 22.14-yr Hale cycle and the 19.86-yr synodic cy-

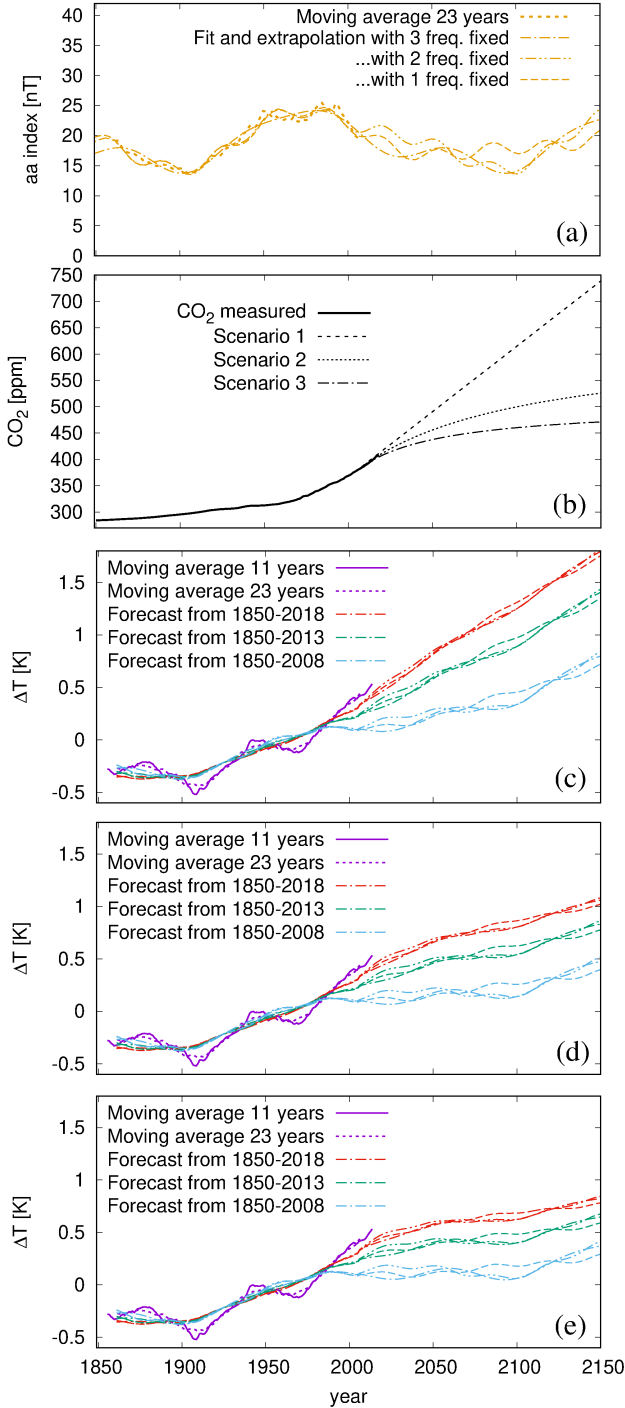


Figure 9: Climate predictions until 2150. (a) 23-year moving average of the aa-index, and three 3-frequency fits to it, extrapolated until 2150. (b) Three scenarios for CO₂ concentration. (c) Temperature forecasts for the 1st CO₂ scenario (dashed curve in (b)), for the three pairs of w_{aa} and w_{CO_2} resulting from regression with end year 2018 (red), 2013 (green), 2008 (blue). Each of the coloured bundles comprise the three different 3-frequency fits from (a). (d) Same as (c), but for the second CO₂ scenario with a mild decarbonization scheme (dotted line in (b)). (e) Same as (c), but for third CO₂ scenario with a radical decarbonization (dash-dotted line in (b)).

cle of Jupiter and Saturn which governs the motion of the Sun around the barycenter of the solar system. Note that, apart from first ideas (Javaraiah, 2003; Sharp, 2013; Solheim, 2013; Wilson, 2013), the spin-orbit coupling that is necessary to translate the orbital motion of the Sun into some dynamo-relevant internal forcing, is yet far from understood. In our model, the Suess-de Vries acquires a clear (beat) period of 193 years which is in the lower range of usual estimates (but see Ma and Vaquero (2020)). The situation with the Gleissberg cycle(s) was less clear: those appeared as doubled and tripled frequencies of the Suess-de Vries cycle, but also as independent frequencies resulting from beat periods of other synodes of Jovian planets with the Schwabe cycle (see Fig. 10 in Stefani, Stepanov and Weier (2020)). Further below, this vagueness of the Gleissberg cycle(s) will be factored in when fitting and extrapolating the aa-index. Lately, in Stefani, Stepanov and Weier (2020) we have tried to explain the transitions between regular and irregular intervals of the solar dynamo (the “supermodulation” as defined by Weiss and Tobias (2016)) in terms of a transient route to chaos.

With those preliminaries, we will now fit the aa-index over the last 170 years in order to extrapolate it into the future. We assume that we have safely left the irregular period of the solar dynamo, as reflected in the Little Ice Age which can be considered as the latest link in the (chaotic) chain of Bond events (Bond *et al.*, 2001). Guided by our (double-)synchronization model, and encouraged by Ma and Vaquero (2020) who had indeed derived an 195-yr cycle in the quiet (regular) interval from 800-1340, we keep this Suess-de Vries period fixed to 193 years in all fits. Concerning the Gleissberg-type cycle(s) we will be less strict, though. In the first version, we fix the two (half and tripled) periods of 96 and 65 years, for the second one we only fix the 96 years period, and for the third one we will keep both Gleissberg cycles undetermined.

In the interval between 1850-2150, the results of those three different 3-frequency fits are presented in Fig. 9a, together with the (fitted) 23-year averaged aa-index data between 1850-2007. Evidently, all three curves approximate the original data reasonably well, and all show a similar extrapolation with a long decay until 2100, and a recovery afterwards. This behaviour is quite similar to the prediction of Bucha and Bucha (1998) (their Figure 14) as well as with the variety of predictions by Lüdecke, Weiss and Hempelmann (2015). The differences between the three fits mainly concern the high frequency part; whereas the version with three frequencies being fixed is the smoothest, the other two fits comprise some stronger wiggles. This simply reflects the fact that the Gleissberg cycle is more vague than the Suess-de Vries cycle. In the following we will always work with all three curves obtained, hoping that they constitute a representative variety for the future of the aa-index.

3.2. Some scenarios

Thus prepared, we consider now three different CO₂ scenarios (Fig. 9b), for each of which we further take into ac-

count the three predictions for the aa-index as just discussed, as well as the three optimal combinations of weights for the aa-index and CO₂ as derived in the previous section. Deliberately, we restrict our forecasts until 2150, admitting that neither the CO₂ trend nor the aa-index are seriously predictable beyond that horizon.

Let us start with the simple case¹ of an unabated linear extrapolation of the recent CO₂ trend to rise by 2.5 ppm annually (upper curve in Fig. 9b), which would bring us to a value 736 ppm in 2150 (still steeper trends are not completely ruled out, but perhaps not that realistic given the recent worldwide reduction commitments). For this scenario, Fig. 9c shows three red, green, and blue bundles of curves, each comprising the three different fits of the aa-index as discussed above. The red bundle (“hot”) corresponds to the red solution in Fig. 7, with a rather high CO₂-sensitivity of 1.5 K and an aa-sensitivity of 0.017 K/nT. The green bundle (“medium”) corresponds to the green solution of Fig. 7 based on sensitivities of 1.2 K and 0.022 K/nT. The blue bundle (“cool”) corresponds to 0.6 K and 0.032 K/nT.

We see that in 2100 the “hot” variant leads to a temperature anomaly of $\Delta T = 1.3$ K which is 0.9 K above the average $\Delta T \approx 0.4$ K from the first decade of this century. The “medium” and “cool” curves are flatter, leading to $\Delta T = 0.9$ K and $\Delta T = 0.4$ K, respectively. However, for those cases to be of any relevance, an imminent drop of the temperature would be required to reach the corresponding curves before they can continue as flat as shown.

The second scenario (dotted line in Fig. 9b) assumes a slowly decreasing upward trend of the CO₂ concentration towards the end of the 21st century, with a hypothetical time dependence

$$\text{CO}_2 = [382 + 2.5(t - 2007)/(1. + (t - 2007)/100)] \text{ ppm}$$

reaching a final value of 529 ppm in 2150. The resulting red, green and blue curves in Fig. 9d show a rather flat behaviour.

The last (and rather unrealistic) CO₂ scenario (dash-dotted line of Fig. 9b) assumes a radical decarbonization path with

$$\text{CO}_2 = [382 + 2.5(t - 2007)/(1. + (t - 2007)/50)] \text{ ppm}.$$

The resulting temperature curves (Fig. 9e) are basically constant throughout the end of our forecast horizon.

4. Conclusions

This work has revived the tradition of correlating solar magnetic field data with the terrestrial climate as pioneered by Cliver, Boriakoff and Feynman (1998) and Mufti and Shah (2011). Just as these authors, we have found an empirical correlation coefficient between the aa-index and ΔT with remarkably high values ranging from 0.8 until 0.96, which points to a significant influence of solar variability on the climate. Our modest innovation was to employ a multiple (double) regression analysis, with the logarithm of atmo-

spheric CO₂ concentration as the second independent variable, whose pre-factor corresponds to an (instantaneous) climate sensitivity of the TCR type. For a lengths of the centered moving average window of 25 years we have identified optimal parameter combinations leading to adjusted R^2 values of around 87 per cent. Depending on whether to include or not include the data from the last decade, the regression gave climate sensitivity values from 0.6 K up to 1.6 K (per $2 \times \text{CO}_2$), and values from 0.032 K/nT down to 0.017 K/nT for the corresponding sensitivity on the aa-index.

Ironically, if interpreted as 1.1 ± 0.5 K, the derived climate sensitivity range turns out to have (nearly) the same ample 50 per cent error bar as the “official” ECS value (3 ± 1.5 K), which we had criticized in the introduction. Yet, in view of the impressive 95 per cent correlation (obtained for the restricted period 1850–2008) we believe the correct climate sensitivity to be situated somewhere in the lower half of that range. This “bias” is also supported by the fact that during the last years an intervening strong El Niño, a positive PDO, and a positive AMO, have all conspired to raise the temperature to significantly higher values than what would be expected from the sole combination of aa-index and CO₂. With the upcoming switch to La Niña conditions, and the imminent return of the PDO and AMO into their negative phases, we expect a significant temperature drop for the coming years, which then might re-establish the strong correlation between aa-index and ΔT . At any rate, the next decade will be decisive for distinguishing between climate sensitivity values in the lower versus those in the upper half of the derived range. In this sense we are more optimistic than Love *et al.* (2011) who believed that we “...would have to patiently wait for decades before enough data could be collected to provide meaningful tests...”. Given the high correlation for most of the past 170 years, and the good correspondence with the results of recent satellite-borne measurements (Feldman *et al.*, 2015; Rentsch, 2019), our “bets” are clearly on the lower half of that range.

Based on those estimates, we have also presented some cautious climate predictions for the next 130 years. With the derived share of the solar influence reaching values between 30 and 70 per cent, such predictions depend critically on a correct forecast of the solar dynamo (in addition to that of CO₂, of course). Following our recent work towards a self-consistent planetary synchronization model of short- and medium-term cycles of the solar dynamo, we have extrapolated some simple 3-frequency fits of the aa-index to the data from the last 170 years into the next 130 years. Apart from intrinsic variabilities of such forecasts (mainly connected with the vagueness of the Gleissberg-type cycle(s)), we prognosticate a general decline of the aa-index until 2100, which essentially reflects the 200-years Suess-de Vries cycle. Such a prediction presupposes that we have indeed left the irregular solar dynamo episode (corresponding to the Little Ice Age, the latest “Bond event”) and that we will further remain in a regular phase of solar activity (Weiss and Tobias, 2016; Stefani, Stepanov and Weier, 2020), similar to that between 800 and 1340 (Ma and Vaquero, 2020). Of

¹While we do not refer here to IPCC’s Representative Concentration Pathways, this case has some similarity to their RCP 6.0, at least until 2100.

course, we have to ask ourselves whether our prediction of a declining aa-index could be completely wrong, with the Sun eventually becoming even “hotter” in the future, thus adding to the warming of CO₂. While such a scenario cannot be completely ruled out, we consider it as not very likely, given that the solar activity at the end of the 20th century was perhaps the highest during the last 8000 years (Solanki *et al.*, 2004), and that it has declined ever since.

As for the CO₂ trend, we have considered three scenarios, comprising an unfettered 2.5 ppm annual increase until 2150, as well as one soft and one radical decarbonization scheme. Even in the “hottest” case considered, we find only a mild additional temperature rise of less than 1 K until the end of this century, while all other cases result in flatter curves in which the heating effect of increasing CO₂ is widely compensated by the cooling effect of a decreasing aa-index. Whatever the rationale of the advocated 2 K goal might be, it will likely be maintained even without any drastic decarbonization measures. Apart from that, we also advise that any imminent temperature drop (due to the turn of ENSO, PDO and AMO into their respective negative phases) should not be mistaken as, and extrapolated to, a long-lasting downward trend (Abdussamatov, 2015).

In this work, we have focused exclusively on a quasi-instantaneous, i.e. TCR-like climate sensitivity on CO₂. As for ECS, we agree with Knutti *et al.* (2017) who opined that “(k)nowing a fully equilibrated response is of limited value for near-term projections and mitigation decisions” and that “(t)he TCR is more relevant for predicting climate change over the next century”. In view of the millennial relaxation time scale underlying the concept of ECS, we fear that - perhaps much too soon - the huge Milankovic drivers will cool down mankind’s hubris of being able to significantly influence the terrestrial climate (in whatever direction).

Data availability

The sea surface temperature data HadSST.4.0.0.0 data were obtained from <http://www.metoffice.gov.uk/hadobs/hadsst4> on November 27, 2020 and are © of British Crown Copyright, Met Office (2020).

The aa-index data between 1868 and 2010 were obtained from NOAA under ftp://ftp.ngdc.noaa.gov/STP/GEOMAGNETIC_DATA/AASTAR/.

Monthly aa-index data between 2011 and 2019 were obtained from the website of the British Geological Survey www.geomag.bgs.ac.uk/data_service/data/magnetic_indices/aaindex.html.

CO₂ data were obtained from <ftp://data.iac.ethz.ch/CMIP6/input4MIPs/UoM/GHGConc/CMIP/yr/atmos/UoM-CMIP-1-1-0/GHGConc/gr3-GMNHSH/v20160701>.

Declaration of competing interest

The author declares that he has no known competing financial interests or personal relationships that could have appeared to influence the work reported in this paper.

Acknowledgment

This work was supported in frame of the Helmholtz - RSF Joint Research Group “Magnetohydrodynamic instabilities”, contract No HRSF-0044. It has also received funding from the European Research Council (ERC) under the European Union’s Horizon 2020 research and innovation programme (grant agreement No 787544). I’m very grateful to André Giesecke, Sebastian Lüning, Willie Soon, Fritz Vahrenholt and Tom Weier for their valuable comments on an early draft of this paper.

5. References

References

- Abdussamatov, H., 2015. Current long-term negative average annual energy balance of the Earth leads to the new little ice age. *Thermal Science* 19, Suppl. 2, 279-288.
- Arrhenius, S., 1906. Die vermutliche Ursache der Klimaschwankungen. *Medd. Kungl. Vetenskapsakad. Nobelinstit.* 1(2), 1-10.
- Bindoff, N.L. et al., 2013. Detection and Attribution of Climate Change: from Global to Regional. IPCC AR5 WG1 Ch10.
- Bond, G., Kromer, B., Beer, J., Muscheler, R., Evans, M.N., Showers, W., Hoffmann, S., Lotti-Bond, R., Hajdas, I., Bonani, G., 2001. Persistent solar influence on North Atlantic climate during the Holocene. *Science* 294, 2130.
- Bucha, V., Bucha, V. Jr., 1998. Geomagnetic forcing of changes in climate and in the atmospheric circulation. *Journal of Atmospheric and Solar-Terrestrial Physics* 60, 145-169.
- Callendar, G. S., 1938. The artificial production of carbon dioxide and its influence on temperature”, *Quarterly. Journal of the Royal Meteorological Society* 64, 223-240.
- Charney, J. et al., 1979. Carbon dioxide and climate: A scientific Assessment (National Academy of Sciences Press).
- Charlson, R.J., Lovelock, J.E., Andreae, M.O., Warren, S.C., 1987. Oceanic phytoplankton, atmospheric sulphur, cloud albedo and climate. *Nature* 326, 655-661.
- Cliver, C.W., Boriakoff, V., Feynman, J., 1998. Solar variability and climate change: Geomagnetic aa index and global surface temperature. *Geophysical Research Letters* 25, 1035-1038.
- Cliver, C.W., Boriakoff, V., Bounar, K.H., 1998. Geomagnetic activity and the solar wind during the Maunder Minimum. *Geophysical Research Letters* 25, 897-900.
- Connolly, R. et al., 2021. How much has the Sun influence Northern hemisphere temperature trends. An ongoing debate. *Research in Astronomy and Astrophysics*, submitted.
- Cook, J. et al., 2016. Consensus on consensus: a synthesis of consensus estimates on human-caused global warming. *Environmental Research Letters* 11, 048002.
- Courtillot, V., Gallet, Y., Le Mouél, J.-L., Fluteau, F., Genevey, A., 2007. Are there connections between the Earth’s magnetic field and climate? *Earth and Planetary Science Letters* 253, 328-339.
- Dicke, R.H., 1978. Is there a chronometer hidden deep in the Sun? *Nature* 276, 676.
- Egorova, T., Schmutz, W., Rozanov, E., Shapiro, A.I., Usoskin, I., Beer, J., Tagirov, R.V., Peter, T., 2018. Revised historical solar irradiance forcing. *Astronomy and Astrophysics* 615, A85.
- Feldman, D.R., Collins, W.D., Gero, P.J., Torn, M.S., Mlawer, E.J., Shipper, T.R., 2015. Observational determination of surfaced radiative forcing by CO₂ from 2000 to 2010. *Nature* 519, 339-343.
- Georgieva, K., Kirov, B., Koucka Knizova, P., Mosna, Z., Kouba, D., Asenovska, Y., 2012. Solar influence on atmospheric circulation. *Journal of Atmospheric and Solar-Terrestrial Physics* 90-91, 15-21.
- Gray, L.J. et al., 2010. Solar influence on climate. *Reviews of Geophysics* 48, 1-53.
- Friis-Christensen, E., Lassen, K., 1991. Length of the solar cycle: an in-

- indicator of solar activity closely associated with climate. *Science* 254, 698-700.-381.
- Haigh, J.D., 1994. The role of stratospheric Ozone in modulating the solar radiative forcing of climate. *Nature*, 370, 544-546.
- Hanel, R.A., Conrath, B.J., 1970. Thermal emission spectra of the Earth and atmosphere from the Nimbus 4 Michelson Interferometer Experiment. *Nature* 228, 143.
- Hart, M. 2015. Hubris: The Troubling Science, Economics, and Politics of Climate Change. Compleat Desktops.
- Hoyng, P., 1996. Is the solar cycle timed by a clock? *Solar Physics* 169, 253.
- Hoyt, D.V., Schatten, K.H., 1993. A discussion of plausible solar irradiance variations. *Journal of Geophysical Research* 98, 18895-18906.
- Hung, C.-C., 2007. Apparent relations between solar activity and solar tides caused by the planets. *NASA/TM-2007-214817*.
- Javaraiah, J., 2003. Long-Term Variations in the Solar Differential Rotation. *Solar Physics*, 212, 23-49.
- Kennedy, J.J., Rayner, N.A., Atkinson, C.P., Killick, R.E., 2019. An ensemble data set of sea surface temperature change from 1850: the Met Office Hadley Centre HadSST.4.0.0.0 data set. *J. Geophys. Res.: Atmosph.* 124, 7719-7763.
- Knutti, R., Rugenstein, M.A.A., Hegerl, G.C., 2017. Beyond equilibrium climate sensitivity. *Nature Geosci.* 10, 727-736.
- Krivova, N.A., Vieira, L.E.A., Solanki, S., 2010. Reconstruction of solar spectral irradiance since the Maunder minimum. *Journal of Geophysical Research: Space Physics*, 115, A12112.
- Labitzke, K., van Loon, H., 1988. Associations between the 11-year solar cycle, the QBO and the atmosphere. Part 1: The troposphere and stratosphere in the northern hemisphere in winter. *Journal of Atmospheric and Terrestrial Physics* 50, 197-206.
- Laubereau, A., Iglev, H., 2013. On the direct impact of the CO₂ concentration rise to the global warming. *EPL* 104, 29001.
- Lean, J.L., Rind, D.H., 2008. How natural and anthropogenic influences alter global and regional surface temperatures: 1889 to 2006. *Geophysical Research Letters* 35, L18701.
- Lean, J.L., 2010. Cycles and trends in solar irradiance and climate? *WIREs Climate Change* 1, 111-121.
- Lewis, N., Curry, J., 2018. The Impact of Recent Forcing and Ocean Heat Uptake Data on Estimates of Climate Sensitivity. *J. Climate* 31, 6051-6071.
- Lindzen, R.S., 2020. An oversimplified picture of the climate behavior based on a single process can lead to distorted conclusions. *Eur. Phys. J. Plus* 135, 462.
- Love, J.J., Mursula, K., Tsai, V.C., Perkins, D.M., 2012. Are secular correlations between sunspots, geomagnetic activity, and global temperature significant? *Geophysical Research Letters* 38, L21703.
- Lüdecke, H.-J., Weiss, C.O., Hempelmann, A., 2015. Paleoclimate forcing by the solar De Vries/Suess cycle. *Climate of the Past Discussions* 11, 279-305.
- Ma, L., Vaquero, J.M., 2020. New evidence of the Suess/de Vries cycle existing in historical naked-eye observations of sunspots. *Open Astronomy* 29, 28.
- Mantua, N.J., Hare, S.R., 2002. The Pacific Decadal Oscillation. *J. Oceanography* 58, 35-44.
- Mayaud, P.-N., 1972. The aa indices: A 100-year series characterizing the magnetic activity. *Journal of Geophysical Research* 77, 6870-6874.
- Mufti, S., Shah, G.N., 2011. Solar-geomagnetic activity influence on Earth's climate. *Journal of Atmospheric and Solar-Terrestrial Physics* 73, 1607-1615.
- Nevanlinna, H., Kataja, E., 1993. An extension of the geomagnetic activity index series aa for two solar cycles (1844-1868). *Geophys. Res. Lett.* 20, 2703-2706.
- Okhlopkov, V.P., 2016. The gravitational influence of Venus, the Earth, and Jupiter on the 11-year cycle of solar activity. *Mosc. Univ. Phys. Bull* 71, 440.
- Parker, E.N., 1999. Sunny side of global warming. *Nature* 399, 416-417.
- Petrovay, K., 2010. Solar cycle prediction. *Liv. Rev. Sol. Phys.* 7, 6.
- Pulkkinen, T.I., Nevanlinna, H., Pulkkinen, P.J., Lockwood, M., 2001. The Sun-Earth connection in time scales from years to decades and centuries. *Space Science Reviews* 95, 625-637.
- Reid, G., 1987. Influence of solar variability on global sea surface temperatures. *Nature* 329, 142-143.
- Rentsch, C.P., 2019. Radiative forcing by CO₂ observed at top of atmosphere from 2002-2019. *arXiv:1911.10605*.
- Roy, I., Asikainen, T., Maliniemi, V., Mursula, K. 2016. Comparing the influence of sunspot activity and geomagnetic activity on winter surface climate. *J. Atmos. Sol.-Terr. Phys.* 149, 167-179.
- Scafetta, N., West, I.M., 2007. Phenomenological reconstructions of the solar signature in the Northern Hemisphere surface temperature records since 1600. *Journal of Geophysical Research: Atmospheres* 112, D24S03.
- Scafetta, N., West, I.M., 2008. Is climate sensitive to solar variability. *Physics Today*, 61(3),50-51.
- Scafetta, N., 2012. Does the Sun work as a nuclear fusion amplifier of planetary tidal forcing? A proposal for a physical mechanism based on the mass-luminosity relation. *J. Atmos. Sol.-Terr. Phys.* 81-82, 27.
- Scafetta, N., Willson, R.C., 2014. ACRIM total solar irradiance satellite composite validation versus TSI proxy models. *Astrophysics and Space Science*, 350, 421-442.
- Sharp, G., 2013. Are Uranus and Neptune responsible for solar grand minima and solar cycle modulation? *Int J. Astron. Astrophys.* 3, 260.
- Shaviv, N.J., Veizer, J., 2003. Celestial driver of Phanerozoic climate? *GSA Today*, 13(7),4-10.
- Silverman, V., Harnik, N., Matthes, K., Lubis, S.W., Wahl, S., 2018. Radiative effects of ozone waves on the Northern Hemisphere polar vortex and its modulation by the QBO. *Atmos. Chem. Phys.* 18, 6637-6659.
- Soden, B.J., Held, I.M., 2006. An assessment of climate feedbacks in coupled ocean-atmosphere models. *J. Clim.* 19, 3354-3360.
- Solanki, S.K., 2002. Solar variability and climate change: is there a link? *Astronomy & Geophysics*, 43, 5.9-5.13.
- Solanki, S.K., Usoskin, I.G., Kromer, B., Schüssler, M., Beer, J., 2004. Unusual activity of the Sun during recent decades compared to the previous 11,000 years. *Nature* 431, 1084-1087.
- Solheim, J.-E., Stordahl, K., Humlum, O., 2012. The long sunspot cycle 23 predicts a significant temperature decrease in cycle 24. *Journal of Atmospheric and Solar-Terrestrial Physics* 80, 267-284.
- Solheim, J.-E., 2013. The sunspot cycle length - modulated by planets? *Pattern Recogn. Phys.* 1, 159.
- Soon, W.H., Posmentier, E.S., Baliunas, S.L., 1996. Inference of solar irradiance variability from terrestrial temperature changes, 1880-1993: An astrophysical application of the Sun-climate connection. *Astrophysical Journal* 472, 891-902.
- Soon, W.H., Posmentier, E.S., Baliunas, S.L., 2000. Climate hypersensitivity to solar forcing? *Ann. Geophysicae* 18, 583-588.
- Soon, W.H., Baliunas, S.L., Posmentier, E.S., Okeke, P., 2000. Variations of solar coronal hole area and terrestrial lower tropospheric air temperature from 1979 to mid-1998: astronomical forcings of change in earth's climate? *New Astron.* 4, 563-579.
- Soon, W., Conolly, R., Conolly, M., 2015. Re-evaluating the role of solar variability on Northern Hemisphere temperature trends since the 19th century. *Earth-Science Reviews* 150, 409-452.
- Stefani, F., Giesecke, A., Weber, N., Weier, T., 2016. Synchronized helicity oscillations: A link between planetary tides and the solar cycle? *Solar Physics* 291, 2197-2212.
- Stefani, F., Galindo, V., Giesecke, A., Weber, N., Weier, T., 2017. The Tayler instability at low magnetic Prandtl numbers: chiral symmetry breaking and synchronizable helicity oscillations. *Magnetohydrodynamics* 53, 169-178.
- Stefani, F., Giesecke, A., Weber, N., Weier, T., 2018. On the synchronizability of Tayler-Spruit and Babcock-Leighton type dynamos. *Solar Physics* 293, 12.
- Stefani, F., Giesecke, A., Weier, T., 2019. A model of a tidally synchronized solar dynamo. *Solar Physics* 294, 60.
- Stefani, F., Giesecke, A., Seilmayer, M., Stepanov, R., Weier, T., 2020. Schwabe, Gleissberg, Suess-de Vries: Towards a consistent model of planetary synchronization of solar cycles. *Magnetohydrodynamics* 56,

- 269-280.
- Stefani, F., Beer, J., Giesecke, A., Gloaguen, T., Seilmayer, M., Stepanov, R., T. Weier, 2020. Phase coherence and phase jumps in the Schwabe cycle. *Astron. Nachr.* 341, 600-615.
- Stefani, F., Stepanov, R., Weier, T., 2020. Shaken and stirred: When Bond meets Suess-de Vries and Gnevyshev-Ohl. *Solar Physics* (submitted); arXiv:2006.08320
- Steinhilber, F., Beer, J., Fröhlich, C., 2009. Total solar irradiance during the Holocene. *Geophysical Research Letters* 36, L19704.
- Svalgaard, L., Cliver, E.W., Kamide, Y., 2005. Sunspot cycle 24: Smallest cycle in 100 years? *Geophys. Res. Lett.* 32, L01104.
- Svensmark, H., Friis-Christensen, E., 1997. Variations of cosmic ray flux and global cloud coverage - A missing link in solar-climate relationship. *Journal of Atmospheric and Solar-Terrestrial Physics*, 59, 1225-1232.
- Svensmark, H., Enghoff, M.B., Shaviv, N.J., Svensmark, J., 2017. Increased ionization supports growth of aerosols into cloud condensation nuclei. *Nature Communications* 8, 2199.
- Tinsley, B.A., 2000. Influence of solar wind on the global electric current, and inferred effects on cloud microphysics, temperature, and dynamics in the troposphere. *Space Science Review* 94, 231-258.
- Tinsley, B.A., 2008. The global atmospheric electric circuit and its effects on cloud microphysics. *Reports on Progress in Physics* 71, 66801-66900.
- Vahrenholt, F., Lüning, S., 2020. Unerwünschte Wahrheiten: Was Sie über den Klimawandel wissen sollten. Langen-Müller.
- Veretenenko, S., Ogurtsov, M.G., 2020. Influence of Solar-geophysical factors on the state of the stratospheric polar vortex. *Geomagnetism and Aeronomy* 60, 974-981.
- Vos, H., Brüchmann, C., Lücke, A., Negendank, J. F. W., Schleser, G. H., Zolitschka, B., 2004. in: *Climate in Historical Times: Towards a Synthesis of Holocene Proxy Data and Climate Models*, eds. H. Fischer, T. Kumke, G. Lohmann, G. Floser, H. Miller, H. Storch, GKSS School of Environmental Research, 293.
- Wang, Y.-M., Lean, J.L., Sheeley, N.R.Jr., 2009. Modelling the Sun's magnetic field and irradiance since 1713. *Astrophysical Journal* 625, 522.
- Weber, W., 2010. Strong signatures of the active Sun in 100 years of terrestrial insolation data. *Ann. Phys. (Berlin)* 522, 372
- Weber, N., Galindo, V., Stefani, F., Weier, T., 2015. The Tayler instability at low magnetic Prandtl numbers: between chiral symmetry breaking and helicity oscillations. *New J. Phys.* 17, 113013.
- Weiss, N.O., Tobias, S.M., 2016. Supermodulation of the Sun's magnetic activity: the effects of symmetry changes. *Mon. Not. Roy. Astron. Soc.* 456, 2654.
- Wilson, I.R.G., 2008. Does a spin-orbit coupling between the Sun and the Jovian planets govern the solar cycle? *Publ. Astron. Soc. Austr.* 25, 85.
- Wilson, I.R.G., 2013. The Venus-Earth-Jupiter spin-orbit coupling model. *Pattern Recogn.Phys.* 1, 147.
- van Wijngaarden, Happer, W., 2020. Dependence of Earth's Thermal Radiation on Five Most Abundant Greenhouse Gases. arXiv:2006.03098.
- Wyatt, M. G., Kravtsov, S., Tsonis, A. A., 2012. Atlantic Multidecadal Oscillation and Northern Hemisphere's climate variability. *Climate Dynamics* 38, 929-949.
- Zherebtsov, G.A., Kovalelenko, V.A., Molodykh, S.I., Kirichenko, K.E., 2019. Solar variability manifestations in weather and climate characteristics. *Journal of Atmospheric and Solar-Terrestrial Physics.* 182, 217-222.